Scientific African 17 (2022) e01355

Contents lists available at ScienceDirect

Scientific African

journal homepage: www.elsevier.com/locate/sciaf

Fracture mechanics of carbon steel under different carbon monoxide and dioxide gas mixture conditions in water

J.W. van der Merwe[a,b], M. du Toit[b,c], D.E.P. Klenam[a,d,*], M.O. Bodunrin[a]

[a] School of Chemical and Metallurgical Engineering, University of the Witwatersrand, Johannesburg, South Africa
[b] Department of Materials Science and Metallurgical Engineering, University of Pretoria, South Africa
[c] School of Mechanical, Materials, Mechatronic and Biomedical Engineering, Faculty of Engineering and Information Sciences, University of Wollongong, Australia
[d] Academic Development Unit, Faculty of Engineering and the Built Environment, University of the Witwatersrand, Johannesburg, South Africa

ARTICLE INFO

Article history:
Received 27 February 2022
Revised 24 June 2022
Accepted 30 August 2022

Editor: DR B Gyampoh.

Keywords:
Stress-corrosion cracking
Carbon steel
Carbon monoxide
Carbon dioxide
Fracture mechanics
Crack growth rate
Stress intensity threshold

ABSTRACT

The results of carbon steel stress-corrosion cracking experiments in a CO-CO_2-H_2O environment at varying gas mixtures are presented. The fracture mechanics of carbon steel were investigated in distilled water under CO-CO_2 combinations of various compositions. For each mixture, the subcritical rates of crack propagation and thresholds for stress intensity were established. Using an applied electrochemical potential, the effects of cathodic and anodic polarization on carbon steel were examined. At a low-stress intensity threshold of 3 MPa$\sqrt{m}$, cracking was caused in a 50% gas mixture. The stress intensity threshold was double that of the 50%CO. Low dissolved oxygen content was reported at 1% CO, with a threshold of 15 MPa$\sqrt{m}$. As a result, increasing CO had the opposite effect on the stress intensity threshold. Cathodic polarization reduced the susceptibility to cracking and the growth rates of subcritical cracks ranged from 10^{-10} to 10^{-9} ms^{-1}. The underpinning stress corrosion mechanisms are investigated further, as well as their consequences in different CO-CO_2-H_2O environments.

Introduction

Coal is the second contributor to energy generation accounting for ~30-40% of the world's energy consumption [1]. Coal gasification is the process of generating electricity through the chemical reaction of CO and CO_2 with significant use of water during the process [1,2]. This leads to the production of syngas during the process and the by-product is highly corrosive wastewater, which is transported using carbon steel pipes for recycling and reuse as cooling agents. The steel pipes operate under high-pressure conditions and are detrimental to structural integrity. As a result, corrosion and stress corrosion cracking-related challenges are prevalent during coal gasification [3–5].

Abbreviations: DCB, Double Cantilever Beam; DO, Dissolved Oxygen; SCC, Stress Corrosion Cracking; KISCC, Critical Stress Intensity for SCC.

* Corresponding author.
E-mail address: desprimus@gmail.com (D.E.P. Klenam).

https://doi.org/10.1016/j.sciaf.2022.e01355

Table 1
Nominal composition of the A516 steel.

Element	Al	B	C	Co	Cr	Cu	V	Mn
wt%	0.009	0.002	0.22	0.01	0.01	0.01	0.01	1.03
Element	Mo	N_2	Nb	Ni	P	S	Ti	Si
wt%	0.01	0.007	0.004	0.02	0.009	0.003	0.001	0.29

Stress corrosion cracking (SCC) is the deterioration or degradation of a metallic material due to the combined (synergetic) effects of a harsh and corrosive atmosphere or environment [6], tensile stresses above a certain threshold and susceptibility of the material to cracking [7–9]. The effects of these factors can lead to catastrophic failure hampering structural integrity. Carbon steels are susceptible to SCC and hydrogen embrittlement, especially in $CO/CO_2/H_2O$ environments [7–11]. In CO_2 dominated environment, the corrosion of carbon steels produces siderite ($FeCO_3$) which is passive but influenced by pH, the chemistry of the holding liquid and carbon concentration [9,12,13]. Though siderite acts as a passive layer on the carbon steel, any mechanical agitation or chemical dissolution exposes the fresh steel surface, promoting metal dissolution via a localized corrosion mechanism. This creates corrosion pits which are stress raisers nucleating new cracks, while old ones propagate. Other factors that affect the corrosion mechanisms include dissolving iron and oxygen contents showing various polymorphs of rust with distinct colouration [14].

Structural assessment of carbon steels exposed to $CO\text{-}CO_2\text{-}H_2O$ environment is essential to avert any catastrophe. Data from this process can be used to select design parameters for pressure vessels, pipelines and "fit-for-service" scenarios and evaluations. It also provides insights into the relationship between stress intensity and crack propagation from applied and residual stresses. By understanding the fracture mechanics in SCC inducing environments, critical parameters such as K_{ISCC} and crack propagation rate thresholds can be derived for best practices.

In this paper, the effect of varying CO and CO_2 concentrations on crack propagation rates of typical carbon steel was investigated. The concentrations of CO were varied at 50%, 9% and 1% CO with CO_2 being the balance. These gas concentrations were chosen to determine the embrittling environment in CO rich concentrations. This is to verify the stress intensity thresholds for SCC. The stress intensity thresholds are also essential in post-weld heat treatments, lowering residual stress states during the welding process [3,8,10]. The reduction in the concentration of CO to ~1% is to estimate the effects of temperature and dissolved oxygen concentration and how it compares to a CO-rich environment. This is to determine the SCC mechanism of the metal in a lean CO concentration. The effects of low partial pressure at low CO concentration were also studied to understand its overarching mechanism on SCC.

Experiments were done to ascertain the rate of cracking at 1% concentration of CO at varying temperatures of 25°C and 45°C [15–17]. Effects of dissolved oxygen in H_2O at low CO were also determined, as it is essential to the rate of crack propagation. The effects of externally applied potential on an SCC mechanism were also investigated. Comparable results have been observed for steels with cracking occurring between -575 and -450 mV using silver-silver chloride electrodes [15–17]. Cracking plateaued at ~ -475 mV for all gas mixtures tested. These test conditions are important in evaluating the effects and contributions of CO to the SCC mechanism. In this paper, the aim is to ascertain and discuss the effects of crack propagation rates and the thresholds for stress intensity on SCC mechanism of carbon steel under various gas mixtures. The samples were cathodically and anodically polarised to correlate and compare with polarisation characteristics and crack growth rates. Perspectives on the fracture mechanics of the polarised steels under the mixed gas conditions are also provided.

Experimental procedure

Materials

The A516 steel which is typically used for pressurized vessels, with compositions given in Table 1 was used for this investigation. The compositions were analysed using a typical Leco Carbon/Sulphur spectrometer.

Water preparation

Low and high dissolved oxygen concentrations were prepared using distilled water. Dissolved oxygen at low concentration was prepared by bubbling nitrogen through distilled water in a vessel for about 60 minutes. For the high concentration of dissolved oxygen, bubbles of air were sent through the container reaching 8 ppm of O_2 was reached. The distilled water was then pressurized at the right $CO\text{-}CO_2$ mixture.

Specimen preparation and configuration

Double cantilever beam (DCB) specimens were prepared, and tests were done in an autoclave (Fig. 1). Test temperatures from room temperature (~25°C) to ~45°C were applied. Above room temperature, extra heating was provided by an au-

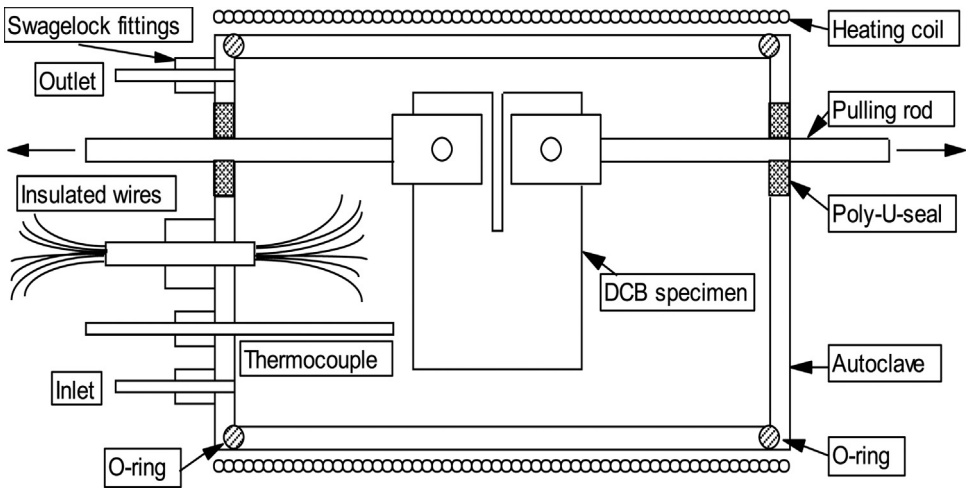

Fig. 1. A schematic diagram of the autoclave used for the experiments.

toclave. Caution was taken by folding the autoclave to prevent the interference of electromagnetic fields, which could be deleterious to the experimental setup, especially the measurement of crack depth.

To measure the crack propagation rates, a potential drop technique was used. This was done by passing constant unit ampere current through the sample while measuring the potential deviations on top of the specimen and the origin of cracks. Detail of the setup is given in supplementary material (Fig. SM1). The ratio of the measured potential drops and the crack origins were used to estimate the crack length. Initial calibrations of the system were done before the experiments commenced.

Stress intensity thresholds were estimated using the DCB specimens based on the ASTM E399 – 83 standards and recommended guidelines (Fig. SM2). The configurations of the samples were in agreement with the linear elastic fracture mechanics standardization and practices, which is the main technique used in this investigation. This was also mainly due to the embrittling environment in which the tests were done. The experiments were done for ~14 hours at a nominal load.

Plane strain fracture toughness (K_Q) of the samples were calculated using Eqs. (1 and 2). The width and thickness of the test samples used in this study are 50 mm and 12 mm respectively. The terms of the equations are defined as:

P_Q = load (N);

B = thickness in mm;

W = width in mm; a = Critical crack length in mm.

$$K_Q = \left(\frac{P_Q}{B\sqrt{W}}\right).f\left(\frac{a}{W}\right) \tag{1}$$

$$f\left(\frac{a}{W}\right) = \frac{\left(2+\frac{a}{W}\right)\left(0.866+4.64\frac{a}{W}-13.32\frac{a^2}{W^2}+14.72\frac{a^3}{W^3}-5.6\frac{a^4}{W^4}\right)}{\left(1-\frac{a}{W}\right)^{\frac{3}{2}}} \tag{2}$$

A ratio of $2.5(\frac{KQ}{\sigma\gamma s})^2$ for most alloys has been proven to be greater than both the thickness (B) and the crack length (a) of the alloys and thus K_Q equating to K_{ISCC}. Hence this relation was adopted to determine the K_{ISCC} of A516 steel under the test conditions.

Environmental variations and applied potential

Stress corrosion cracking tests were done at varying conditions of gas mixtures: 50%Co – 50%CO_2, 9%Co – 91%CO_2 and 1%CO – 99%CO_2 concentrations. For the 50%Co – 50%CO_2 concentration, the tests were performed over the entire stress intensity spectrum. For the 9%CO - 91%CO_2 and 1%CO - 99%CO_2 concentrations, emphasis is on the effects of dissolved oxygen (DO) concentration and temperature on the crack propagation rates was critical. Dissolved oxygen concentrations of 0.1 and 8 ppm O_2 and temperatures of 25°C and 45°C were selected as shown in Table 2. The effect of loading rate on the 50%Co – 50%CO_2 and 1%CO – 99%CO_2 was also studied. For the experimental setup, a Pt electrode was positioned in the autoclave as a counter electrode to control the electrochemical potential, which was measured using the Ag-AgCl reference electrode with a Luggin probe. The samples were polarised between -650 mV and -490 mV with Ag-AgCl electrode. The Ag-AgCl electrode is indicated as SSC in the polarisation curves presented in section 3. The slow strain rate used to evaluate SCC was 10^{-6} s^{-1}, whereas a 0.1 mV/s corrosion scan rate was used.

Table 2
Experimental parameters used for the experiment.

Test	Temperature (°C)	Concentration of dissolved oxygen (ppm)
1	**25**	**8**
2	**25**	**0.1**
3	**45**	**8**
4	**45**	**0.1**

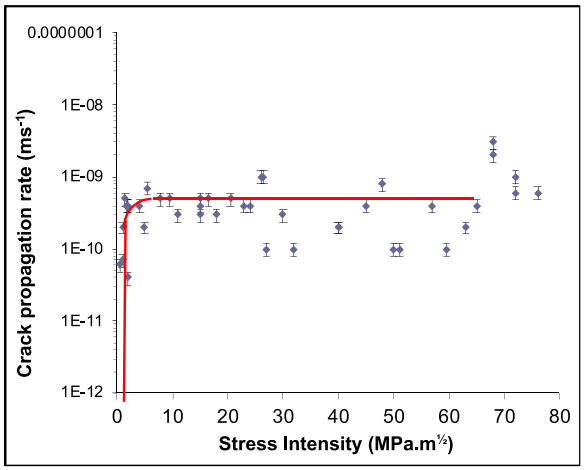

Fig. 2. Relationship between rate of crack propagation and stress intensity of A516 steel under 50%CO - 50%CO_2 at 800 kPa and 45°C.

Table 3
Results from tests performed with 9%CO and 91%CO_2-H_2O.

Temperature (°C)	DO (ppm)	K_{ISCC} (MPa$\sqrt{m}$)	da/dt (ms^{-1})
25	0.1	7	5×10^{-11}
25	8	5	8×10^{-10}
45	0.1	10	8×10^{-10}
45	8	6	1×10^{-9}

Results

Fracture mechanics behaviour of A516 in 50%CO- 50%CO_2 – H_2O

The critical stress intensity for SCC, K_{ISCC} value was determined (Fig. 2) where the crack propagation rate is as a function of stress intensity. The K_{ISCC} was exceptionally low, ~3 MPa$\sqrt{m}$ and crack propagation rate plateaued at 4×10^{-10} ms^{-1}. The rates of crack propagation were independent on stress intensity beyond ~3 MPa$\sqrt{m}$, as shown by the scatter in the data. A gentle increase in the crack propagation rates was observed as a function of loading and the critical rate of crack propagation was measured upon loading.

Fracture mechanics of A516 steel in 9%CO – 91%CO_2-H_2O

The fracture toughness of the A516 steel exposed to water with 9%CO and 91%CO_2-H_2O were studied at 25°C and 45°C and in 0.1 and 8 ppm concentrations of dissolved oxygen. The summary of results is given in Table 3, whereas the fracture mechanical characteristics are shown in the supplementary materials (Fig.s SM3 and SM4).

The subcritical rate of crack propagation for the A516 steel in 9%CO – 1%CO_2 mixtures and at 8 ppm of dissolved O_2 at 25°C showed a considerable scatter ranging from 2×10^{-12} to 5×10^{-11} ms^{-1}. This was also observed for the same condition of dissolved gas. At ~45°C, the subcritical rates of crack propagation showed scatter above ~1×10^{-12} ms^{-1}. Though the stress corrosion cracking tests were done to ascertain the effect of dissolved oxygen and temperature on the fracture mechanics behaviour of the steel, the results were inconclusive. Thus, more experimental work will be required to elucidate any underpinning factors influencing the mechanisms and to arrive at definitive conclusions.

The notable observations from this work was that, with high dissolved oxygen concentration, the threshold for stress intensity for cracking was not affected much by the increase in temperature, however, higher critical crack propagation rates were found. At the lower dissolved oxygen concentration, the subcritical crack propagation was higher with an increase

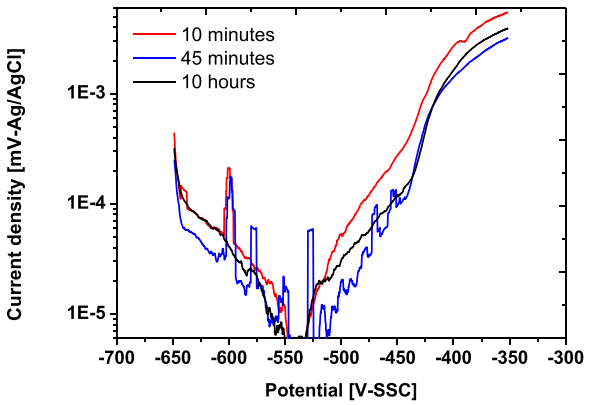

Fig. 3. Polarization behaviour of A516 steel tested in 50%CO – 50%CO_2 gas mixtures and at 45°C and 800 kPa, with a 0.1 mV/s scan rate after being held from 10 minutes to 10 hours for OCP.

in temperature, but not enough tests were performed to establish the effect on the stress intensity threshold. Hence, the underpinning mechanisms could not be established at this current stage.

Fracture mechanics of A 516 steel in 1%CO- 99%CO_2 – H_2O

Under the 1% CO- 99% CO_2 – H_2O condition, the dissolved oxygen and the testing temperature were varied within the three different conditions (environments). At 45°C, effects of the dissolved oxygen were at high and low oxygen contents (Fig. SM5). For 0.1 ppm oxygen concentration, the K_{ISCC} was 4 MPa$\sqrt{m}$, whereas the subcritical rate of cracking for crack propagation was 1×10^{-10} ms^{-1}. A relatively high rate of crack growth was observed above 50 MPa$\sqrt{m}$ stress intensity and at $\sim 3 \times 10^{-9}$ ms^{-1}.

In the case of the 25°C, the oxygen content was kept at 0.1 ppm and the K_{ISCC} was 13 MPa$\sqrt{m}$ (Fig. SM6). The subcritical crack propagation rate was 8×10^{-10} ms^{-1}, and then increased to 3×10^{-9} ms^{-1} at ~51 MPa$\sqrt{m}$. The magnitude of crack propagation rates beyond ~51 MPa$\sqrt{m}$ was not determined. No experiments were performed at these stress intensities due to impracticality considering relatively low intensities are more applicable especially for typical pressurized vessels.

With increasing temperature to ~45°C and at 0.1 ppm dissolved oxygen concentration, the K_{ISCC} reduced drastically to ~4 MPa$\sqrt{m}$ with a simultaneous drop in the subcritical rate of crack growth to 5×10^{-10} ms^{-1}. This is a degree of magnitude lower than values obtained for high dissolved oxygen concentration at the same test temperature.

Fracture mechanics behaviour of A516 in 50%CO - 50%CO_2 – H_2O with externally applied potential

Polarisation of the test samples affected the rate of crack propagation and the critical stress intensity for SCC. For test specimens polarised to -490 mV, the K_{ISCC} for SCC at a test temperature of 45°C was ~15 MPa$\sqrt{m}$ with subcritical rates of crack propagation in the domain of 2×10^{-10} ms^{-1} (Fig. SM7). At polarization tests of −470 mV, the rate of crack propagation rate was 1×10^{-10} ms^{-1}, whereas a rate of 4×10^{-10} ms^{-1} was achieved at −430 mV. Relatively low K_{ISCC} for SCC (10 MPa$\sqrt{m}$) and critical rate of crack propagation below 1×10^{-9} ms^{-1} was observed at polarisation potential of −480 mV. For very low polarization potential (−620 mV), the K_{ISCC} for SCC and critical rate of crack propagation was 15 MPa$\sqrt{m}$. and 1×10^{-11} ms^{-1} respectively. The potential range where cracking would be expected with varying open current potential exposures is given by the polarisation curve in Fig. 3. It should be noted that the corrosion potential falls within the range of -525 to -550 mV rather than having a definite value, but this is of little significance as the influence of applied potential on SCC was the main concern of this study. The steel was cathodic at −620 mV and anodic at −480 and −490 mV, where cracking was expected within the passive range.

The effect of potential on the fracture mechanics of steel in 50% CO - 50%CO_2 gas mixtures at 25°C and 800 kPa showed a remarkable increase in K_{ISCC}, from 11 MPa$\sqrt{m}$ to above 35 MPa$\sqrt{m}$ (Fig. SM8). The critical rate of crack propagation decreased significantly from $\sim 2 \times 10^{-10}$ ms^{-1} to 1×10^{-10} ms^{-1}. The critical crack propagation rate at -620 mV and test temperatures of 25°C was relatively higher than for the same applied potential at 45°C.

At the stress intensity of 20 MPa$\sqrt{m}$ and with increasing anodic polarisation (Fig. SM9), there was a significant drop in applied potential. The rate of crack propagation at ~20 MPa$\sqrt{m}$ showed a discernible drop in applied potential while increasing the anodic polarisation side (Fig. SM9). No distinct crack propagation rates were observed at 25°C and 45°C test temperatures, whereas the propagation rates were extremely high for the anodic potentials at 25°C and above -550mV, which was unexpected. This warrants further investigation to establish the overarching mechanisms. However, simultaneous effects of stresses, electrolytic medium and any possible hydrogen evolution at room temperature at the crack tip could be contributing factor.

Discussion

Fracture mechanics of A516 in 50%CO – 50%CO_2 – H_2O

Low values of stress intensity thresholds for SCC makes it difficult for the design of pressurized vessels and structures, and to operate them at tight stress conditions and allowable thresholds. The low-stress intensity thresholds in 50%CO – 50%CO_2 – H_2O mixture are indicative of the sensitivity of A516 steel to SCC. In most of these environments, the instability of the passive layer was highly unstable and impervious resulting in significant material degradation due to the combined effects of residual or applied stresses and the highly corrosive environment. Thus, the pressurized steel was severely prone to stress corrosion-induced cracking. In our previous article on typical steels used for manufacturing pressure vessels [10], microstructural evidence of these environmentally induced cracks have been reported.

In this study, the measured crack propagation rate showed scatter which is attributed to the strain rate at the crack tip. In the 50%CO – 50%CO_2 – H_2O, the rate of cracking was estimated to corrosion rate of ~12 mm/yr, showing severe cracking phenomenon in pressure vessels and pipelines. The current response measurements are indicative of the stress intensity thresholds for which for SCC could occur.

Fracture mechanics of A516 in 9%CO- 91%CO_2 – H_2O

Under the 9%CO – 91%CO_2 – H_2O, high dissolved oxygen concentration and high temperature were the most severe conditions considered. These conditions were similar for the gas mixtures investigated previously. At 25°C, the stress intensity threshold for crack propagation decreased significantly due to dissolved oxygen concentration. However, the subcritical rate of crack propagation remained constant with increased dissolved oxygen. At 45°C, the K_{ISCC} decreased due to dissolved oxygen, whereas the subcritical rate of crack propagation did not show any substantial increase, although the trend increased with increased dissolved oxygen. At the dissolved oxygen of 0.1 ppm, there was significant decrease in rate of crack propagation due to the temperature effect and the threshold for cracking remained the same. At 8 ppm of dissolved oxygen, the temperature effect on the threshold stress intensity for SCC was negligible. Increasing temperature increased the sub-critical crack propagation rate exponentially.

As the temperature is slightly increased, the rates of subcritical crack propagation under the 9%CO – 91%CO_2 – H_2O condition are also increased and kinetically driven. Hence, the overarching mechanism at the crack tip was driven from a kinetic standpoint of the reaction which is typical for corrosion-controlled reactions.

Fracture mechanics of steel in 1%CO- 99%CO_2 – H_2O

For the 1%CO – 99%CO_2 – H_2O gas mixture, the system is mainly pure CO_2. However, CO was the main component inhibiting the SCC of the A516 steel. For the SCC mechanism, 1%CO is sufficient for adequate passivation, but a slight deviation was observed in the trends [18–22]. It is suggestive of the possibility of mechanisms other than the threshold of the CO gas could have induced cracking, as is mostly the case for hydrogen embrittlement. It is also possible that the CO_2 could have provided some catalytic effect in increasing the rate of SCC under the dissolved oxygen and temperature at which the test was conducted [18–22]. The SCC is influenced mainly by dissolved oxygen and test temperature [23]. Thus, while the test temperature increased the K_{ISCC} value, the dissolved oxygen content led to an increased subcritical crack propagation rate at stress intensities above the K_{ISCC} value.

Carbon monoxide is the main component that cause corrosion inhibition of steel especially at very high carbon dioxide contents [24,25]. According to SCC mechanism, this limit is enough for adequate passivation to cracking [24,25]. There could be another mechanism inducing the cracking process, which warrants some experimental work and investigation. Also, the CO_2 could have had a discernible effects on SCC as observed for hydrogen embrittlement of steels [26–30]. At 8 ppm of dissolved oxygen concentration, subcritical crack propagation rates were very high. At low temperatures, the subcritical crack propagation rates were fairly constant, whereas the stress intensity threshold was reduced to ~ 16 MPa$\sqrt{m}$.

Corrosion inhibition of steel is generally not dependent on the partial pressures of CO gas [23]. This holds if sufficient time is allowed for inhibition to occur. Regardless of the gas mixtures and the partial pressures, there is no major shift in the cathodic and anodic curves as well as polarization characteristics and corrosion densities. Generally, corrosion inhibition is very slow at low CO concentrations and the passivation is generally kinetically-controlled and temperature driven. The passivation rate can be lowered by increasing the critical stress intensity factor [18–22,27–30].

High dissolved oxygen content increases the susceptibility to SCC by controlling the free corrosion potential of the system [18–22]. This results in a very high rate of crack growth, but do not affect the critical stress intensity. Thus reducing dissolved oxygen does not increase the stress intensity threshold for SCC. Increasing the stress intensity factor is vital and retards crack propagation beyond limitations in the cracking environment. Generally, at the crack tip, the critical strain rate breaks the film and also the overarching parameter that increases the rate of crack propagation. Thus, the driving force for high crack propagation rates under the SCC condition [18–22,27–30].

Fracture mechanics of A516 in 50%CO- 50%CO_2 – H_2O with an external potential

Stress corrosion cracking can be significantly reduced by the anodic and cathodic polarization under 50%CO – 50%CO_2 – H_2O condition [26,31–33], but the susceptibility to SCC generally shows a different trend. The subcritical crack propagation rate for the 50%CO – 50%CO_2 – H_2O condition followed a similar trend as the previous conditions, which was $\sim 1 \times 10^{-10}$ - 2×10^{-10} ms^{-1}. Comparing this to the open circuit tests, it is a slightly reduced propagation rate. Higher K_{ISCC} was observed at −490 mV (Ag-AgCl electrode) than that for OCP. This trend was pronounced at a potential of −650 mV (Ag-AgCl electrode). Minor variation in the potential applied led to significant reduction in crack propagation, which was also observed at relatively high stress intensity thresholds. Cathodic polarization was the driven force that enabled SCC at −650 mV with the crack tip being the main contributing factor, especially in the presence of hydrogen that dissociated from the water.

Conclusions

The fracture mechanics of carbon steel under mixed gases of CO-CO_2 compositions in water was studied. Based on the experimental approach, results and discussions, the following conclusions were drawn. With the increase in CO, the stress intensity threshold dropped to 3 $MPa\sqrt{m}$. At 9%CO-91%CO_2 and 1% CO-99%CO_2, the stress intensity threshold was around 8 $MPa\sqrt{m}$, for all levels of dissolved oxygen tested, except for 1% CO at 25°C the threshold was measured at ~17 $MPa\sqrt{m}$.

The rates of subcritical crack propagation were all between 1×10^{-10} and 1×10^{-9} ms^{-1}, except for 45°C with 8 ppm dissolved oxygen where it increased to 2×10^{-9} ms^{-1}. The K_{ISCC} value of 1 $MPa\sqrt{m}$ was found in aqueous solutions at 45°C in the case of 1%CO and 99%CO_2 mixture. Dissolved oxygen at 45°C increased crack propagation to $1 \times 10^{-9} ms^{-1}$. The K_{ISCC} value decreased steadily with increasing dissolved oxygen in the distilled water. The effect of dissolved oxygen on the rate of subcritical crack propagation was negligible. The temperature increased the rate of sub-critical crack propagation irrespective of the amount of dissolved oxygen. The temperature had a minute or negligible effect on the overall threshold for stress intensity needed for SCC. The K_{ISCC} of 35 $MPa\sqrt{m}$ at an applied potential of −650 mV Ag – AgCl electrode is applied, whereas a K_{ISCC} of 15 $MPa\sqrt{m}$ was observed at a potential of −490 mV Ag – AgCl electrode and at 45°C. Thus, minute changes in potential greater than −490 mV increased resistance to SCC.

Funding

There is no funding for this work.

Declaration of Competing Interest

The authors declare that they have no known competing financial interests or personal relationships that could have appeared to influence the work reported in this paper.

Supplementary material

Supplementary material associated with this article can be found, in the online version, at doi:10.1016/j.sciaf.2022.e01355.

References

[1] Z. Chen, X. Zhang, W. Han, L. Gao, S. Li, Energy analysis on the process with integrated supercritical water gasification of coal and syngas separation, Appl. Therm. Eng. 128 (2018) 1003–1008.
[2] G. Oh, H.W. Ra, S.M. Yoon, T.Y. Mun, M.W. Seo, J.G. Lee, S.J. Yoon, Syngas production through gasification of coal water mixture and power generation on dual-fuel diesel engine, J. Energy Inst. 92 (2019) 265–274.
[3] E. Traversa, T. Calderón, Electrochemical investigation on carbon steel behaviour in CO-CO2-H2O environment for the interpretation of the SCC mechanism, Mater. Corros. 42 (1991) 35–40.
[4] M.G. Hebsur, A brief survey of attempts to develop corrosion/erosion resistant materials for coal gasification, Appl. Energy. 15 (1983) 99–126.
[5] W.J. Lochmann, Materials problems in coal gasification and liquefaction, Metall. Trans. A. 9 (1978) 175–181.
[6] M.O. Bodunrin, L.H. Chown, J.W. Van Der Merwe, K.K. Alaneme, C. Oganbule, D.E.P. Klenam, N.P. Mphasha, Corrosion behavior of titanium alloys in acidic and saline media: Role of alloy design, passivation integrity, and electrolyte modification, Corros. Rev. 38 (2020) 25–47.
[7] A. Brown, J.T. Harrison, R. Wilkins, Trans-granular stress corrosion cracking (SCC) of ferritic steels, Corros. Sci. 10 (1970) 547–548.
[8] M. Kowaka, S. Nagata, Stress corrosion cracking of mild and low alloy steels in CO-CO2-H2O environments, Corrosion 32 (1976) 395–401.
[9] M. dos R. Tagliari, P. Craidy, D. Fonseca, M.F. Borges, Stress corrosion cracking of carbon steels on CO2 /H2 O systems, Tecnol. Em Metal. Mater. e Mineração. 18 (2021) 1–14.
[10] J.W. van der Merwe, Environmental and material influences on the stress-corrosion cracking of steel in H-CO-CO2 solutions, Int. J. Corros. (2012) 1–13.
[11] R.W. Bowman, A.K. Dunlop, J.P. Tralmer, CO/CO2 cracking in inert gas miscible flooding, Corrosion 16 (1977) 28–32.
[12] R. Barker, D. Burkle, T. Charpentier, H. Thompson, A. Neville, A review of iron carbonate (FeCO3) formation in the oil and gas industry, Corros. Sci. 142 (2018) 312–341.
[13] R. De Motte, E. Basilico, R. Mingant, J. Kittel, F. Ropital, P. Combrade, S. Necib, V. Deydier, D. Crusset, S. Marcelin, A study by electrochemical impedance spectroscopy and surface analysis of corrosion product layers formed during CO2 corrosion of low alloy steel, Corros. Sci. 172 (2020) 108666.
[14] D.E.P. Klenam, M.O. Bodunrin, S. Akromah, E. Gikunoo, A. Andrews, F. McBagonluri, Ferrous materials degradation: characterisation of rust by colour-an overview, Corros. Rev. 39 (2021) 297–311.
[15] A. Brown, J.T. Harrison, R. Wilkins, Investigations of stress corrosion cracking of plain carbon steel in the carbon dioxide -carbon monoxide - water system, in: Conf. Stress Corros. Crack. Hydrog. Embrittlement Iron Base Alloy, 1979, pp. 686–695.

[16] L. Nyrkova, S. Melnichuk, S. Osadchuk, P. Lisovyi, S. Prokopchuk, Investigating the mechanism of stress corrosion cracking of controllable rolling pipe steel X70 in near-neutral environment, in: Mater. Today Proc., 2021.
[17] M. Javidi, S. Bahalaou Horeh, Investigating the mechanism of stress corrosion cracking in near-neutral and high pH environments for API 5L X52 steel, Corros. Sci. 80 (2014) 213–220.
[18] R.C. Newman, R.P.M. Procter, Silver jubilee review stress corrosion cracking: 1965-1990, Br. Corros. J. 25 (1990) 259–269.
[19] C.A. Loto, Stress corrosion cracking: characteristics, mechanisms and experimental study, Int. J. Adv. Manuf. Technol. 93 (2017) 3567–3582.
[20] J. Beavers, T.A. Bubenik, Stress corrosion cracking, Trends Oil Gas Corros. Res. Technol. Prod. Transm. 48 (2017) 295–314.
[21] J.R. Galvele, Surface mobility mechanism of stress-corrosion cracking, Corros. Sci. 35 (1993) 419–434.
[22] R.N. Parkins, Predictive approaches to stress corrosion cracking failure, Corros. Sci. 20 (1980) 147–166.
[23] E.E. Heaver, R.F. Sandenbergh, Inhibition of stress corrosion cracking of carbon manganese steels in the CO2-H2O system, in: J.. Costa, A.. Mercer (Eds.), Prog. Underst. Prev. Corros., 1993, pp. 1562–1572.
[24] H. Malik, F. Nawaz, Stress corrosion cracking and electrochemistry of C−Mn steels in CO−CO2−H2O environments, Anti-Corrosion Methods Mater. 52 (2005) 259–265.
[25] E.E. Heaver, Stress corrosion cracking of steels in industrial process environments, 1994.
[26] H. Ma, L. Sun, H. Luo, X. Li, Hydrogen embrittlement of high-strength marine steel as a weld joint in artificial seawater under cathodic polarization, Eng. Fail. Anal. 134 (2022) 106044.
[27] R.E. Smallman, R.J. Bishop, Modern Phys. Metallur. Mater. Eng. (2019).
[28] M.R. Louthan, R.E. Swanson, Material defects, gas purity and hydrogen embrittlement, Int. J. Hydrogen Energy. 10 (1985) 551–554.
[29] S.C. Silva, A.B. Silva, J.A.C. Ponciano Gomes, Hydrogen embrittlement of API 5L X65 pipeline steel in CO2 containing low H2S concentration environment, Eng. Fail. Anal. 120 (2021) 105081.
[30] P. Bai, J. Zhou, B. Luo, S. Zheng, C. Chen, Roles of carbon dioxide and steam on the hydrogen embrittlement of 3Cr tube steel in synthetic natural gas environment, Corros. Eng. Sci. Technol. 53 (2018) 1–10.
[31] L. Yong, L. Zhiyong, F. Endian, C. Zhongyu, Z. Jinbin, The effect of crack tip environment on crack growth behaviour of a low alloy steel at cathodic potentials in artificial seawater, J. Mater. Sci. Technol. 54 (2020) 119–131.
[32] Y. Li, Z. Liu, E. Fan, Y. Huang, Y. Fan, B. Zhao, Effect of cathodic potential on stress corrosion cracking behavior of different heat-affected zone microstructures of E690 steel in artificial seawater, J. Mater. Sci. Technol. 64 (2021) 141–152.
[33] Q. Lu, L. Wang, J. Xin, H. Tian, X. Wang, Z. Cui, Corrosion evolution and stress corrosion cracking of E690 steel for marine construction in artificial seawater under potentiostatic anodic polarization, Constr. Build. Mater. 238 (2020) 117763.